Extreme Mechanics Letters 40 (2020) 100871

Contents lists available at ScienceDirect

Extreme Mechanics Letters

journal homepage: www.elsevier.com/locate/eml

Liquid metal microchannels as digital sensors in mechanical metamaterials

Zachary H. Nick [a], Christopher E. Tabor [b], Ryan L. Harne [a,*]

[a] Department of Mechanical and Aerospace Engineering, The Ohio State University, Columbus, OH 43210, USA
[b] Materials and Manufacturing Directorate, Air Force Research Laboratory, Wright-Patterson AFB, OH 45433, USA

ARTICLE INFO

Article history:
Received 1 May 2020
Received in revised form 10 July 2020
Accepted 10 July 2020
Available online 13 July 2020

Keywords:
Liquid metal
Microchannel
Mechanical metamaterials
Digital sensing
Self sensing
Material assembly

ABSTRACT

This report explores a synthesis of principles from liquid metal-based flexible electronics and mechanical metamaterials. In such new platforms, mechanical deformation couples with liquid metal microchannels to govern electrical conduction by constriction and release of liquid metal embedded in the soft material. The mechanisms that influence the ability to induce such discrete switch electrical phenomena are identified through studies focused on mechanical design, liquid metal oxidation, and stress thresholds. Through strategic selection of such factors, repeatable switch ability is retained for many stress cycles on the metamaterial, although aging of the phenomena is evident through switch thresholds that reduce with cycles prior to potential failure. These discoveries provide new foundations for self-sensing mechanical metamaterials that leverage an interface of liquid metal coalescence and local mechanical deformation to lead to digital signaling abilities in continuously stressed metamaterials.

1. Introduction

Compliant and liquid conductors establish essential foundation for future wearable technologies, reconfigurable circuits, soft robots, and more [1–8]. Gallium-based liquid metals have seen a recent surge of attention due to increased conformability of the liquid phase when synthesized with elastomeric substrates or host structures [9–16]. Strategic use of liquid metal moreover creates opportunity for stress-activated functionality, such as via polymerized liquid metal networks [17] or liquid metal-elastomeric materials [18]. This opportunity to leverage an integration of elastomeric matrix and liquid metal inclusions has uncovered unique self-healing functionality in liquid metal–elastomer composites when subjected to damaging stresses [19]. Studies on liquid metal-based reconfigurable electronics have considered the movement of liquid metal through microscale passages as a means to empower adaptive antennas, responsive circuits, and other compliant switchable electronic networks [20]. In these examples, external pumps are employed to govern the flow and conductivity of the liquid metal [21–23] thus associating pump activation with system functionality. Studies on lattice structures with integrated liquid metal-filled microchannels have exemplified the capabilities of such combination of mechanics and conformal conductive liquid. Boley et al. [24] introduced a 4D printing technique for intricate mechanical lattices capable of 3D shape changes that, when selectively innervated with liquid metal, act as a shape-shifting and tunable patch antenna. Chen et al. [25] created a deposition modeling method to devise scalable and conformal tactile sensing grids with liquid metal microchannels capable of measuring the magnitude and location of an applied force. These recent steps to integrate liquid metal into engineered lattice architectures suggest a broad potential to leverage mechanical design with conformal conductive liquid metal to realize multiple functions in soft engineered matter.

Inspired by these opportunities, this report proposes a concept for reconfigurable electrical circuits based on the mechanical deformation of liquid metal-filled microstructure. In this way, the need for external pumps is eliminated by exploiting intrinsic mechanical stress application from the environment or by material use that results in switchable conductivity of the electrical network. Such principle has been studied recently for *electronic metamaterial* concepts that adapt conductivity on the basis of dynamic loads. Sears et al. [26,27] demonstrated the first combination of such principles using Ag-TPU conductive traces (silver-thermoplastic polyurethane) on TPU metamaterial structures that combined smooth change of conductivity properties according to applied compressive stresses. The smoothly varying conductivity of the Ag-TPU materials resulting from continuously applied strain [26,27] provides first evidence of merging metamaterial mechanics with stretchable electronic materials yielding an analog mode of electrical function. On the other hand, digital operations are the language of many electronic devices that may

* Corresponding author.
E-mail address: harne.3@osu.edu (R.L. Harne).

https://doi.org/10.1016/j.eml.2020.100871
2352-4316/

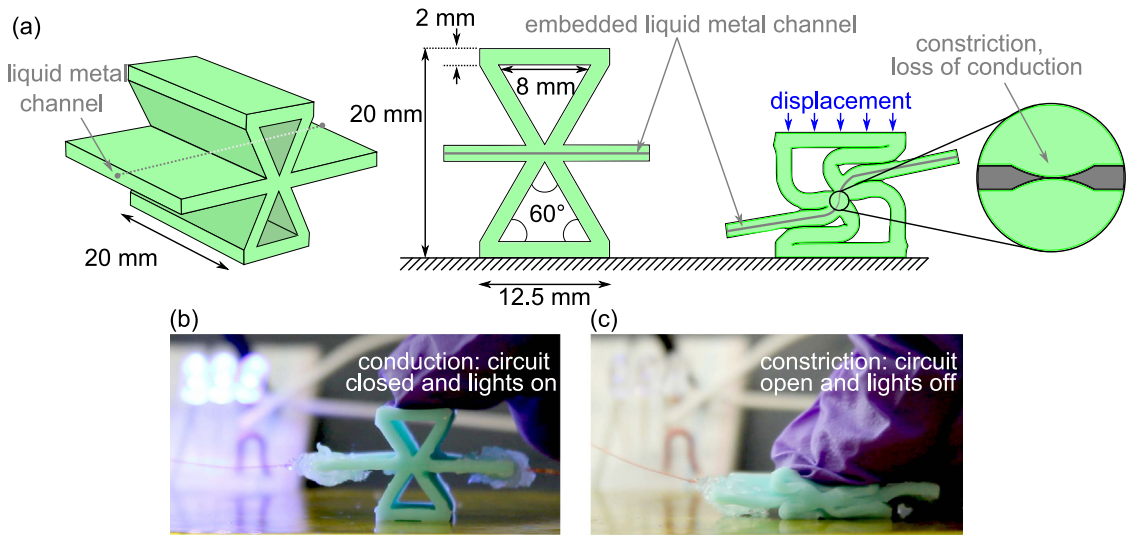

Fig. 1. (a) Metamaterial unit cell illustrating mechanism for channel constriction. (b) LEDs remain lit when connected in series with the unit cell in an undeformed state, whereas (c) an open circuit results when the unit cell is compressed beyond a threshold that constricts liquid metal conduction, leading to switching off of the lights.

interface with the conductive materials. This encourages formulation of flexible electronic materials that may change conductivity in discrete modes. By establishing a method of integrating liquid metal networks within mechanical metamaterials where metamaterial deformation results in discrete change of conductivity, new fundamental concepts of digital logic governed by metamaterial mechanics may be formulated.

Motivated by such opportunities, this report investigates a multifunctional metamaterial concept that yields digital electrical signaling in response to smooth, continuous metamaterial compressive deformation of buckling members. These functionalities are realized simultaneously by introducing void architectures into a bulk elastomer of constant cross-section with a centrally located liquid metal microchannel, Fig. 1. The triangular voids form an X-shaped beam network, similar to the embodiment of metamaterial studied by Bunyan and Tawfick [28] and El-Helou and Harne [29]. A central elastomer ligament passes through the center of the X shape, through which runs a liquid metal-filled microchannel. When compressed, the beam network rotates about the center, leading to a pinching action on the microchannel containing the liquid metal, as shown in Fig. 1a. This constriction of liquid metal terminates the conduction through the microchannel, creating an open circuit. This behavior is shown in Fig. 1b,c where a series connection of the metamaterial unit with an LED matrix turns off the lights once the liquid metal is constricted due to metamaterial compression. When the load is removed, the liquid metal may recoalesce at the pinched region and close the circuit to recover the electrical functionality.

This report studies the liquid metal metamaterial unit to identify the mechanisms involved to induce and control the discrete electrical conductivity behavior observed in the preliminary example of Fig. 1. Having established an understanding of the parametric influences governing the electrical operation, the unit is tiled into a periodic and functionally graded metamaterial to test the working principles observed at the unit level in relation to mechanisms of digital operation at the scale of a material system. The report concludes with a summary of discoveries achieved here and trajectories of continuing research.

2. Fabrication and experimental methods

Throughout this study, the metamaterials and units are fabricated by first casting silicone rubber into 3D printed molds. Acrylonitrile butadiene styrene (ABS) filament is used for the 3D printed (FlashForge Creator Pro) mold negatives. Polymer wire is stretched taut through passages in the molds to create the microchannels. A variety of elastomers are investigated as elastic matrices to contain the liquid metal microchannels, varying broadly in elastic and viscoelastic properties. For the purpose of consistency in this report, we report samples fabricated using a platinum cure silicone rubber (Smooth-On Mold Star 15S, Macungie, Pennsylvania). The rubber is cast in the 3D printed mold and the manufacturer-recommended 4-hour cure time is allowed to pass in atmospheric room conditions prior to demolding. Upon demolding the silicone rubber from the mold, the polymer wire is extracted to reveal a hollow microchannel within the elastomer sample. A syringe with 22-gauge needle is used to inject sodium hydroxide (NaOH, 0.1M) through the empty microchannel. The influence of the NaOH is studied in latter portions of this report. In general, the NaOH solution impedes the liquid metal oxidation. Another syringe then injects liquid metal (Galinstan, GaInSn, Rotometals, San Leandro, California) into the microchannel. Copper wire of 34 gauge is inserted into each microchannel end before sealing the microchannel with additional silicone rubber. The specimen is dried for 24 h prior to experimental study. The unit cell cross-section is 20 mm deep to sufficiently enforce plane strain deformation when the unit is subjected to uniaxial displacement and stress, Fig. 1a.

To analyze the electrical and mechanical properties of the metamaterials and units during applied compressive loads, the samples are examined in a load frame (ADMET eXpert 5600, Norwood, Massachusetts) that actuates a rigid platen. A load cell (PCB 110205A, Depew, New York) attached to the upper platen measures the reactive force from the metamaterial as the sample is uniaxially compressed. During compression, a laser displacement sensor (Micro-Epsilon optoNCDT ILD1700-200, Raleigh, North Carolina) identifies the displacement of the platen and, consequently, the top surface of the metamaterial. The resistance of the liquid metal-filled microchannel is monitored using a voltage divider connected to a 5 V source. Data is recorded and processed in a MATLAB program. Complete experimental detail is provided in the Supporting Information.

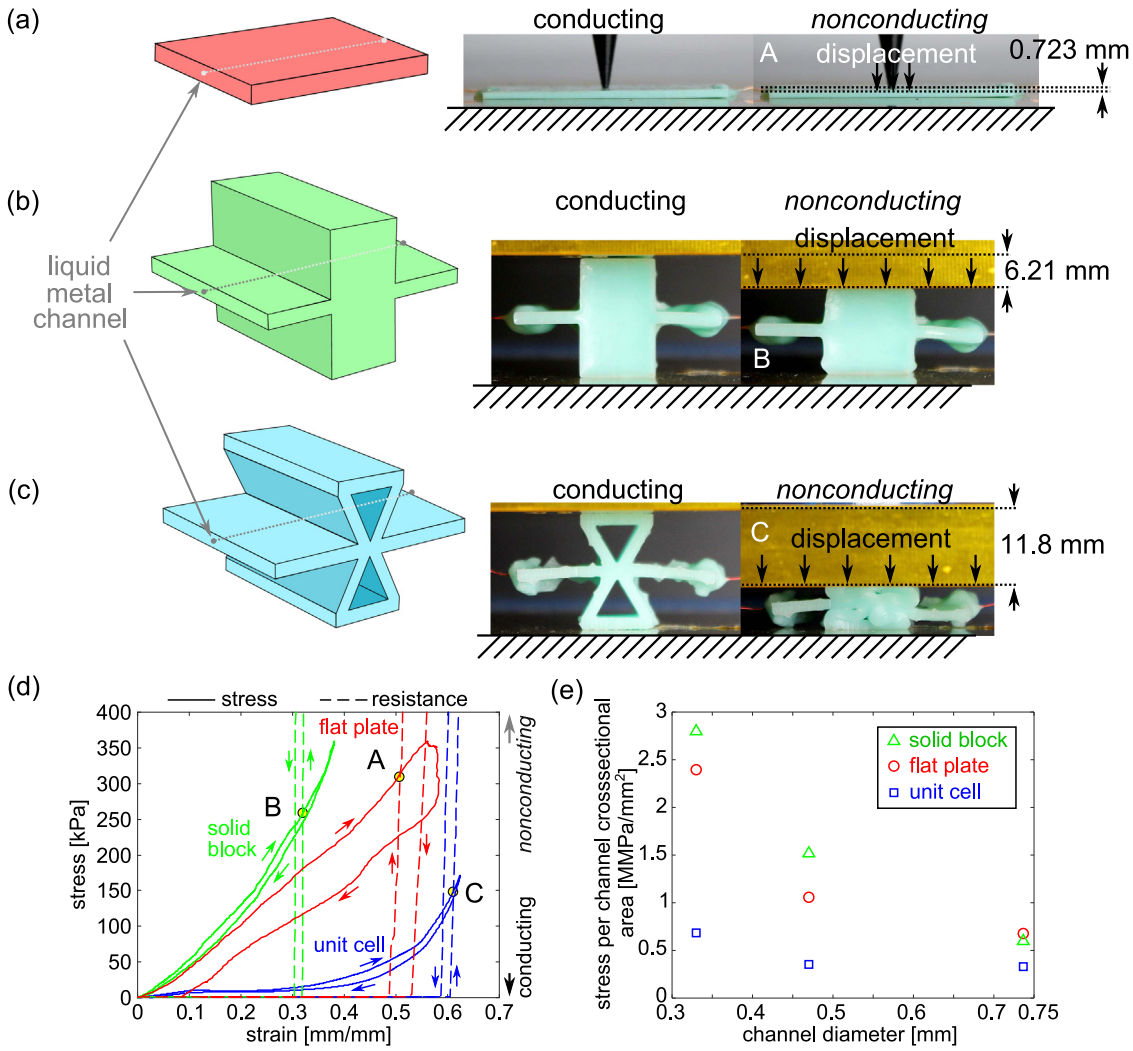

Fig. 2. Schematics and photographs of undeformed and deformed samples exhibiting switchable electrical functionality due to liquid metal microchannel constriction. (a) Flat plate, (b) solid block, and (c) metamaterial unit cell are shown. (d) Uniaxial mechanical properties with circles denoting strains sufficient to eliminate conduction and labels A, B, C that correspond to photographs in (a), (b), (c) respectively. (e) Influence microchannel diameter on stress required to disconnect the circuit.

3. Results and discussion

3.1. Conductivity controlling mechanisms

If constriction is the mechanism by which the electrical conductivity is discretely changed, then it is necessary to assess the relative modes of constriction that may be leveraged. Multiple specimens are fabricated to test the hypothesis of constriction-controlled conductivity. Liquid metal microchannels are embedded in a thin flat plate of silicone rubber, in a solid silicone rubber block of the same net cross-sectional span as the metamaterial unit, and in the X-shaped metamaterial unit, shown in Figs 2a, 2b, and 2c, respectively. The thin flat plate in Fig. 2a has length, width, and thickness of 60 mm (along which the microchannel runs), 30 mm, and 1.5 mm, respectively. The dimensions of the solid rubber block in Fig. 2b are 20 mm height, 10 mm width (along which the microchannel runs), and 20 mm depth. The dimensions of the X-shaped metamaterial unit are described in Section 2. Each specimen type is fabricated with microchannel diameters of 0.330 mm, 0.460 mm, and 0.737 mm. Each experiment runs for one complete loading cycle, which involves compression sufficient to eliminate electrical conduction through the respective microchannel, followed by release of the compressive load. Each step of loading and unloading occurs at a constant rate of 2 mm per minute. The flat plate is uniaxially compressed with a conical indenter at the location of the microchannel, Fig. 2a, while the solid rubber block and X-shaped metamaterial are uniaxially compressed with the flat platen, Fig. 2b, c.

The results in Fig. 2d relate the applied uniaxial displacement with the resulting stress measured at the respective indenter or platen for specimens possessing microchannels of 0.737 mm diameter. Despite the conical indentation at the microchannel location, a high stress of nearly 288 kPa is required to eliminate conduction in the flat plate specimen. This is observed around a displacement of 0.723 mm in Fig. 2d, where the resistance through the liquid metal trace transitions from around 1 Ω to an open circuit. The analogous events to eliminate conductivity for the solid rubber block and metamaterial unit respectively occur for stresses of 256 kPa and 140 kPa and displacements 6.21 mm and 11.8 mm. The physical deformation of each specimen at the moment of loss of conductivity is depicted in Figures 2a,b,c. Upon removal of the applied displacement, each specimen regains conductivity as evidenced by the loading and unloading arrows to indicate the direction of applied displacement in Fig. 2d. These results help to confirm that mechanical constriction of the liquid metal microchannel is the mechanism to eliminate and recover electrical conductivity regardless of the material embodiment.

A normalized stress measure assists in evaluating the influence of microchannel diameter on the stress activation point

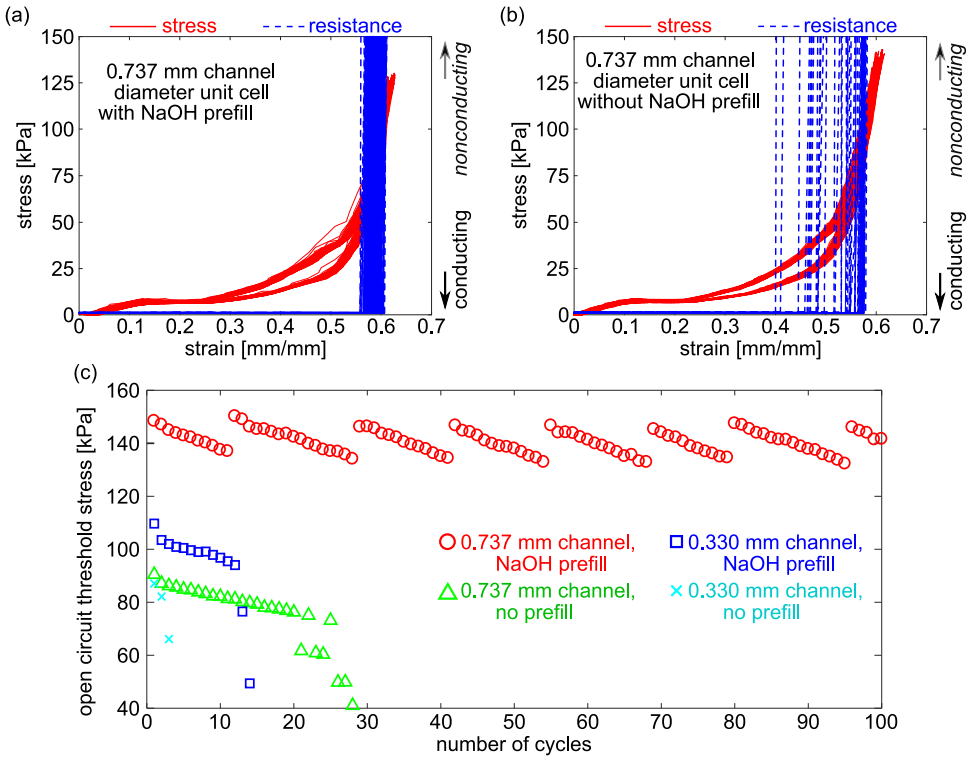

Fig. 3. Uniaxial mechanical properties for unit cell metamaterial (a) with NaOH solution, and (b) without NaOH solution over 100 cycles of loading and unloading. (c) Stress that results in a switch from conducting to nonconducting states for 0.737 mm and 0.330 mm microchannel diameters, with and without NaOH solution.

corresponding to the loss of conductivity. With the increase of microchannel diameter, the stress per microchannel cross-sectional area required to disconnect the liquid metal conduction decreases, Fig. 2e. Moreover, the results in Fig. 2e indicate that the metamaterial unit cell requires less stress per microchannel cross-sectional area to constrict the liquid metal conduit. Since the same mechanism is leveraged in each specimen to eliminate and recover conduction, that is the constriction of the microchannel, the rotation of the unit cell cross-section seen in Fig. 1a may therefore play a role to further locally constrict the microchannel than the more uniform deformation fields observed by the flat plate and solid rubber block specimens. Fig. 2e also reveals that the range of stresses per microchannel cross-sectional area to constrict conduction decreases as the microchannel diameter increases. This indicates that the microchannel diameter is less influential to control the stress required to constrict conduction as channel diameter increases. In other words, the intricate metamaterial unit cell cross-sectional deformation leads to less variation of cross-section normalized stress to control the digital switching functionality than the use of the same constriction mechanisms in flat plate or solid rubber forms.

The uniaxial effective material modulus (or uniaxial stiffness) is observed from Fig. 2d as the slope of the stress–strain profiles. The results reveal that unit cell exhibits varying uniaxial stiffness with change in the applied strain, including slightly negative stiffness after the X-shaped beam networks buckles and rotates, around 0.108 strain. These properties permit favorable functioning in dynamic load environments including vibration and shock [30,31]. By contrast, the flat plate and solid rubber block exhibit quasi-linear effective uniaxial stiffnesses. As a result, the metamaterial unit cell provides advantageous mechanical properties along with the means to discretely switch the passage of electrical signals through the unit based on applied stress, a dual-purpose nature not afforded by the counterpart plate and block.

3.2. Conductive switching longevity

The prefill treatment of NaOH prior to injection of liquid metal is discovered to be a vital contributor to longevity of the reversible switching conductivity properties. With exposure to an oxygenated environment, Ga-based liquid metals form an electrically insulative oxide skin. It is established that NaOH inhibits formation of oxide on Ga liquid metals [32]. Here, the influence of NaOH solution in the microchannel is assessed in detail. A unit cell identical to that studied in Section 3.1 with a 0.737 mm diameter microchannel is prefilled with a NaOH solution and is monitored for a loading and unloading experiment that repeats through 100 cycles. A second unit cell of nominally identical fabrication is used, except no NaOH solution is employed prior to injecting the liquid metal. Fig. 3a shows the mechanical properties of the applied displacement and resulting stress for all 100 cycles of the unit cell prefilled with NaOH solution, along with the electrical resistance that fluctuates between conducting at low stress conditions to non-conducting for high stress conditions. The points at which the conduction switches are not at the same stress and displacement conditions for each cycle, although the distinctions are small for the 100 cycles of evaluation. By contrast, the unit cell without being prefilled with the NaOH solution shows similar mechanical properties yet does not exhibit consistent switching functionality, as seen in Fig. 3b. In fact, only the first 28 of 100 cycles observe the reversible conduction behavior, after which conduction is permanently terminated.

The stresses at which conduction is switched from conducting to non-conducting states are plotted in Fig. 3c as a function of the cycle number. For the case of the 0.737 mm diameter microchannel prefilled with NaOH solution, the cycle-degradation of the switching functionality is apparent. A staircase-type of trend is observed, as well, to be discussed in the following paragraphs. A similarly prolonged working life of the switching functionality is achieved by prefilling a NaOH solution for a 0.330 mm diameter

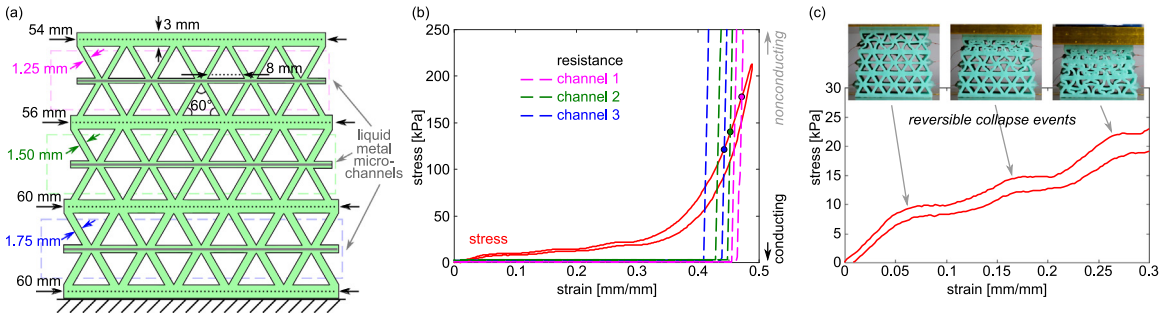

Fig. 4. (a) Cross-section of functionally graded metamaterial assembly. (b) Uniaxial mechanical properties and electrical conductivity for each layer. (c) Uniaxial mechanical properties from 0 to 0.3 strain featuring sequential layer-by-layer collapse.

microchannel unit cell, seen in Fig. 3c. For all cases in Fig. 3c, with the exception of the 0.737 mm microchannel diameter channel unit cell that was prefilled with NaOH solution, the sudden loss of conduction follows a steady decline of the stress required to activate the switch functionality.

These results suggest that larger microchannel diameters coupled to the effect of prefill with NaOH solutions prolongs the repeatable switching function of the liquid metal metamaterial units. There are two potentially related explanations for the longer stress-cycling switching conductivity of the unit cells with NaOH solutions prior to liquid metal filling. Namely, H_2O from the NaOH solution may evaporate or diffuse into the silicone resulting in NaOH crystals forming in the channels. Upon introduction of the liquid metal to the microchannel, the crystalized NaOH may solvate with small amounts of surface bound moisture on the liquid metal oxide skin and chemically remove the oxide. Alternatively, it is also possible that the dissociated NaOH ions in solution partially diffuse into the silicone rubber matrix, as has been seen with other acidic and basic solutions in silicone matrices [33], thereafter permeating back into the liquid metal and removing oxide. Moreover, unit cells without the NaOH solutions may exhibit greater internal surface tractions that prevent the channels from reversibly opening and closing, so that it is possible NaOH serves as a lubricant to the internal channel collapse mechanics. These potential explanations for the role of NaOH prefill solution to prolong the stress-cycling switching conductivity of the unit cell are not mutually exclusive and each may contribute to the observed electrical behavior of the material when under cyclic mechanical stress. Continued investigations are probing these factors to fully elucidate the precise combination of mechanisms culminating in the observed switching behavior.

Measurements for the metamaterial unit with the 0.737 mm diameter liquid metal microchannel with NaOH solution show a staircase type pattern in Fig. 3c. Three samples of this metamaterial unit are fabricated and independently examined (see Supporting Information). Each sample exhibits a similar rise and fall trend of the activation stress, with a slight to minor net decline of the stress required to activate the switch behavior as cycle count increases. The staircase type trend of switching appears analogous to the stick–slip flow of liquid metal characterized by Larsen et al. [34] associated with formation and breaking of liquid metal oxide layers in stress–strain cycling. We propose that the same mechanism governs the conductivity of electrical current through the compressed and released microchannel in the metamaterial units examined here by virtue of similar phenomenological stress and strain conditions.

Probing the detailed mechanisms governing electrical properties of the metamaterials remains an intricate task. Based on the experimental findings, a combination of mechanical stress and oxidation collectively determine the threshold stresses for conduction and loss of conduction during stress cycling of the metamaterial units. Such combined physical mechanisms challenges conventional modeling tools, such as the finite element method. Optical imaging using translucent elastic matrices is also considered as a means to reveal innerworkings of the constriction modality. On the other hand, the oxidation of the liquid metal on the interior walls of the microchannels results in a black residue that obscures direct line-of-sight of the collapsing microchannel. While other conductive liquids not suffering oxidation concerns, such as ionic liquid, may be employed as the conductive medium, the surface chemistry affecting the adhesion of polymer channel walls during compression would greatly differ. Nevertheless, despite fluctuating stress activation trends observed with the current liquid metal and elastomer combination, this study identifies that large microchannel diameters with NaOH solution coatings promote long life cycles of electrical switching functionality.

3.3. Metamaterial assembly and multifunctionality

Given the observations on stress activated insulation in the liquid metal microchannel through the X-shaped unit cell, a metamaterial is fabricated from periodic unit cells that change in beam thickness per layer. Fig. 4a presents a schematic of the functionally graded metamaterial, showing beam thicknesses of 1.25 mm, 1.5 mm, and 1.75 mm per layer. The horizontal elastomer segments are 3 mm thick by virtue of containing 1.6 mm perforated polypropylene to enforce layer by layer compression [29]. Liquid metal microchannels with NaOH solutions and 0.737 mm diameters are applied as shown in Fig. 4a. The electrical conduction through each layer and macroscopic mechanical properties monitored during loading and unloading cycles with results are shown in Fig. 4b.

As the metamaterial is uniaxially compressed, the conduction is switched off in the microchannels for the least uniaxial stress at channel 3, followed by channel 2 for slightly greater stress, and then in channel 1 for still further increase in stress. The stresses at which the electrical disconnections occur are 115 kPa, 131 kPa, and 157 kPa, respectively, for the 3rd, 2nd, and 1st microchannels. During the unloading sequence, the microchannels recover conduction in the reverse order, beginning with channel 1, followed by channel 2, and finally with channel 3. In agreement with the results of Section 3.1, the activation of the switching affect in the functionally graded metamaterial appears to be collectively associated with local and global stress in the distinct layers.

The uniaxial mechanical properties of the metamaterial are shown in detail in Fig. 4c. The results show that collapse of each layer occurs sequentially from the thinnest top layer to the bottom thickest layer. Recovery occurs in the opposite sequence. Because the electrical conduction switching sequence occurs in the opposite layer order for loading and unloading cycles, it may be suggested that the sequence of conduction switching is determined for the functionally graded metamaterial by the

stress field related to the compacted solid. In other words, once all layers collapse in the metamaterial in Fig. 4c, the compacted metamaterial exhibits greater stress in the bottom-most layer since the material is quasi-solid around strains of 40%. Section 3.1 confirmed that solids may also exhibit such electrical switching behaviors, although the metamaterial reduces the absolute stress and relative stress per microchannel cross-sectional area required to induce the switch. As a result, the functionally graded metamaterial exhibits both functional mechanisms that govern conductivity through the liquid metal microchannel. These novel findings of utilizing liquid metal-filled microchannels within mechanical metamaterials for discrete sensing provide a foundation from which more intricate microchannel networks may be implemented across multiple layers of varying thicknesses to yield strain sensitive and strain insensitive sensing [26].

4. Conclusions

This research established a multifunctional metamaterial concept that yields digital electrical signaling in response to smooth, continuous metamaterial compressive deformation of buckling members. It is found that conduction may be discretely controlled through internal microchannel constriction, where constriction thresholds are governed by the stress per microchannel cross-sectional area and the material unit geometry. In addition, repeated use of the discrete switching concept is promoted by larger diameter microchannels that are flushed with NaOH prior to injection of liquid metal in the microchannel. These constituents may be built up into metamaterial systems that leverage versatile mechanical properties coupled with digital signaling capability. By capitalizing on the new discoveries of this research, ongoing studies may uncover further approaches to harness the interface between liquid metal microchannels and metamaterials for self-sensing mechanical soft matter.

Declaration of competing interest

The authors declare that they have no known competing financial interests or personal relationships that could have appeared to influence the work reported in this paper.

Acknowledgment

This research is supported in part by a U.S. Air Force Research Lab Summer Faculty Fellowship.

Appendix A. Supplementary data

Supplementary material related to this article can be found online at https://doi.org/10.1016/j.eml.2020.100871.

References

[1] N. Lu, C. Lu, S. Yang, J. Rogers, Highly sensitive skin-mountable strain gauges based entirely on elastomers, Adv. Funct. Mater. 22 (2012) 4044–4050.
[2] C. Majidi, R. Kramer, R. Wood, A non-differential elastomer curvature sensor for softer-than-skin electronics, Smart Mater. Struct. 20 (2011) 105017.
[3] J. Muth, D. Vogt, R. Truby, Y. Mengüç, D. Kolesky, R. Wood, J. Lewis, Embedded 3D printing of strain sensors within highly stretchable elastomers, Adv. Mater. 26 (2014) 6307–6312.
[4] C. Pang, G. Lee, T. Kim, S. Kim, H. Kim, S. Ahn, K. Suh, A flexible and highly sensitive strain-gauge sensor using reversible interlocking of nanofibres, Nature Mater. 11 (2012) 795–801.
[5] F. Suarez, D. Parekh, C. Ladd, D. Vashaee, M. Dickey, M. Öztürk, Flexible thermoelectric generator using bulk legs and liquid metal interconnects for wearable electronics, Appl. Energy 202 (2017) 736–745.
[6] A. Valentine, T. Busbee, J. Boley, J. Raney, A. Chortos, A. Kotikian, J. Berrigan, M. Durstock, J. Lewis, Hybrid 3D printing of soft electronics, Adv. Mater. 29 (2017) 1703817.
[7] S. Xu, Y. Zhang, L. Jia, K. Mathewson, K. Jang, J. Kim, H. Fu, X. Huang, P. Chava, R. Wang, S. Bhole, Soft microfluidic assemblies of sensors, circuits, and radios for the skin, Science 344 (2014) 70–74.
[8] M. Dickey, Stretchable and soft electronics using liquid metals, Adv. Mater. 29 (2017) 1606425.
[9] B. Blaiszik, A. Jones, N. Sottos, S. White, Microencapsulation of gallium–indium (Ga–In) liquid metal for self-healing applications, J. Microencapsul. 31 (2014) 350–354.
[10] B. Blaiszik, S. Kramer, M. Grady, D. McIlroy, J. Moore, N. Sottos, S. White, Autonomic restoration of electrical conductivity, Adv. Mater. 24 (2012) 398–401.
[11] J. Boley, E. White, G. Chiu, R. Kramer, Direct writing of gallium-indium alloy for stretchable electronics, Adv. Funct. Mater. 24 (2014) 3501–3507.
[12] J. Boley, E. White, R. Kramer, Mechanically sintered gallium–indium nanoparticles, Adv. Mater. 27 (2015) 2355–2360.
[13] M. Dickey, Emerging applications of liquid metals featuring surface oxides, ACS Appl. Mater. Interfaces 6 (2014) 18369–18379.
[14] A. Diebold, A. Watson, S. Holcomb, C. Tabor, D. Mast, M. Dickey, J. Heikenfeld, Electrowetting-actuated liquid metal for RF applications, J. Micromech. Microeng. 27 (2017) 025010.
[15] Z. Farrell, C. Tabor, Control of gallium oxide growth on liquid metal eutectic gallium/indium nanoparticles via thiolation, Langmuir 34 (2018) 234–240.
[16] S. Holcomb, M. Brothers, A. Diebold, W. Thatcher, D. Mast, C. Tabor, J. Heikenfeld, Oxide-free actuation of gallium liquid metal alloys enabled by novel acidified siloxane oils, Langmuir 32 (2016) 12656–12663.
[17] C. Thrasher, Z. Farrell, N. Morris, C. Willey, C. Tabor, Mechanoresponsive polymerized liquid metal networks, Adv. Mater. 31 (2019) 1903864.
[18] A. Fassler, C. Majidi, Liquid-phase metal inclusions for a conductive polymer composite, Adv. Mater. 27 (2015) 1928–1932.
[19] E. Markvicka, M. Bartlett, X. Huang, C. Majidi, An autonomously electrically self-healing liquid metal-elastomer composite for robust soft-matter robotics and electronics, Nature Mater. 17 (2018) 618–624.
[20] J. Dang, R. Gough, A. Morishita, A. Ohta, W. Shiroma, Liquid-metal-based reconfigurable components for RF front ends, IEEE Potentials 4 (2015) 24–30.
[21] D. Hartl, G. Frank, G. Huff, J. Baur, A liquid metal-based structurally embedded vascular antenna: i. concept and multiphysical modeling, Smart Mater. Struct. 26 (2017) 025001.
[22] W. Su, S. Nauroze, B. Ryan, M. Tentzeris, Novel 3D printed liquid-metal-alloy microfluidics-based zigzag and helical antennas for origami reconfigurable antenna trees, in: Proceedings of the 2017 IEEE MTT-S International Microwave Symposium (IMS), Honolulu, Hawaii, USA, 2017.
[23] B. Cumby, G. Hayes, M. Dickey, R. Justice, C. Tabor, J. Heikenfeld, Reconfigurable liquid metal circuits by Laplace pressure shaping, Appl. Phys. Lett. 101 (2012) 174102.
[24] J. Boley, W. van Rees, C. Lissandrello, M. Horenstein, R. Truby, A. Kotikian, J. Lewis, L. Mahadevan, Shape-shifting structured lattices via multimaterial 4D printing, Proc. Natl. Acad. Sci. 116 (2019) 20856–20862.
[25] Y. Chen, Y. Liu, J. Ren, W. Yang, E. Shang, K. Ma, L. Zhang, J. Jiang, X. Sun, Conformable core–shell fiber tactile sensor by continuous tubular deposition modeling with water-based sacrificial coaxial writing, Mater. Des. 190 (2020) 108567.
[26] N. Sears, J. Berrigan, P. Buskohl, R. Harne, Flexible hybrid electronic material systems with programmable strain sensing architectures, Adv. Energy Mater. 20 (2018) 1800499.
[27] N. Sears, J. Berrigan, P. Buskohl, R. Harne, Dynamic response of flexible hybrid electronic material systems, Compos. Struct. 208 (2019) 377–384.
[28] J. Bunyan, S. Tawfick, Exploiting structural instability to design architected materials having essentially nonlinear stiffness, Adv. Energy Mater. 21 (2019) 1800791.
[29] C. El-Helou, R. Harne, Exploiting functionally graded elastomeric materials to program collapse and mechanical properties, Adv. Energy Mater. 21 (2019) 1900807.
[30] D. Restrepo, N. Mankame, P. Zavattieri, Phase transforming cellular materials, Extreme Mech. Lett. 4 (2015) 52–60.
[31] P. Vuyk, S. Cui, R. Harne, Illuminating origins of impact energy dissipation in mechanical metamaterials, Adv. Energy Mater. 20 (2018) 1700828.
[32] R. Bilodeau, D. Zemlyanov, R. Kramer, Liquid metal switches for environmentally responsive electronics, Adv. Mater. Interfaces 4 (2017) 1600913.
[33] G. Li, M. Parmar, D. Kim, J. Lee, D. Lee, PDMS Based coplanar microfluidic channels for the surface reduction of oxidized, Galinstan Lab Chip 14 (2014) 200–209.
[34] R. Larsen, M. Dickey, G. Whitesides, D. Weitz, Viscoelastic properties of oxide-coated liquid metals, J. Rheol. 53 (2009) 1305–1326.

Supporting Information: Liquid metal microchannels as digital sensors in mechanical metamaterials

Zachary H. Nick[1], Christopher E. Tabor[2], and Ryan L. Harne*[1]

[1] Department of Mechanical and Aerospace Engineering, The Ohio State University, Columbus, OH 43210 USA

[2] Materials and Manufacturing Directorate, Air Force Research Laboratory, Wright-Patterson AFB, OH 45433 USA

** Corresponding author: harne.3@osu.edu*

1 Experimental setup

To investigate and understand the conductive switching functionality of the reconfigurable electronic metamaterials, measurements of electrical properties coinciding with mechanical behavior are acquired. The experimental setup consists of a load frame (ADMET eXpert 5600, Norwood, Massachusetts) that uniaxially displaces the specimen. A rigid platen attached to a load cell (PCB 110205A, Depew, New York) interfaces the load cell and specimen by uniaxially compressing and releasing the specimen on a rigid bottom plate. A laser displacement sensor (Micro-Epsilon optoNCDT ILD1700-200, Raleigh, North Carolina) is attached to the upper part of the load frame to monitor the displacement of the moving platen. The copper leads from the specimens are interfaced in a voltage divider circuit to monitor electrical resistance through the liquid metal microchannel. The experimental setup is displayed in Figure S1.

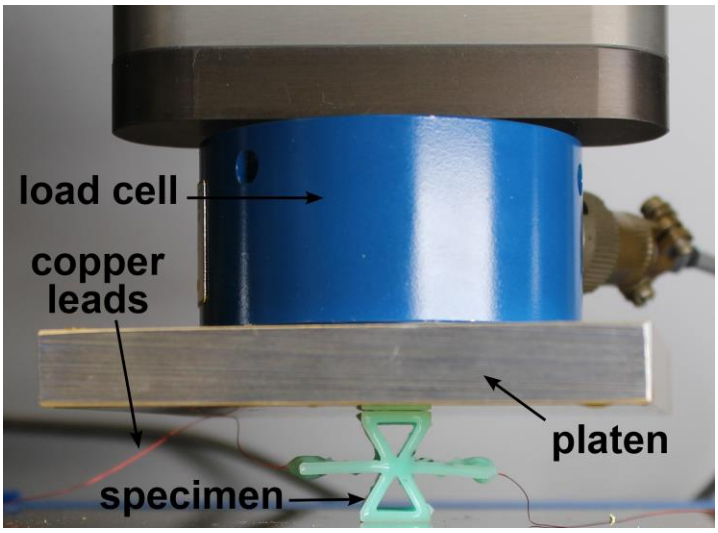

Figure S1. Experimental setup for characterizing mechanical and electrical properties of the specimens.

2 Staircase trends in open circuit threshold stress

To investigate the staircase type pattern of open circuit threshold stress during stress-cycling exhibited by the 0.737 mm microchannel with NaOH prefill, three nominally identical samples of the unit cell are fabricated and examined as outlined in Section 2 of the main text using taut polymer wire of 0.737 mm diameter to create the microchannels. Figure S2 shows the results of stress-cycling the samples in terms of

the open circuit threshold stress per cycle. Each sample displays the staircase type pattern of stress-deactivation degradation. The results confirm that despite NaOH solution prefill, the stick-slip flow of liquid metal occurs. The stick-slip behavior was first characterized by Larsen et al. [1] who found the response to be associated with formation and breaking of liquid metal oxide layers corresponding to stress-strain cycling. The effective elasticity of the oxide coating of the liquid metal varies by orders of magnitude depending on time and strain history [1]. The increase of surface area of the oxide film decreases effective elasticity of the oxide skin, while net increase of oxide increases the apparent elasticity. The variance in initial stress to deactivate conduction may be attributed to the process of prefilling the microchannels with NaOH and potentiality for multiple modes of oxide removal due to the prefill solution. In other words, the initial open circuit threshold stress may be affected by the amount of NaOH retained within a microchannel prior to liquid metal filling, and the amount of time between sealing and testing. Furthermore, as the elasticity and growth of oxides show cycle and strain dependence, the complex interaction between oxide growth from these factors and the continual hydraulically-induced interaction between oxide and NaOH may lead to variance in stress thresholds for opening the circuit in subsequent cycles. Nevertheless, the results reported from data collected in this research are consistent that larger microchannels with NaOH prefill provide conduction switching functionality that is repeatable for greater number of stress cycles.

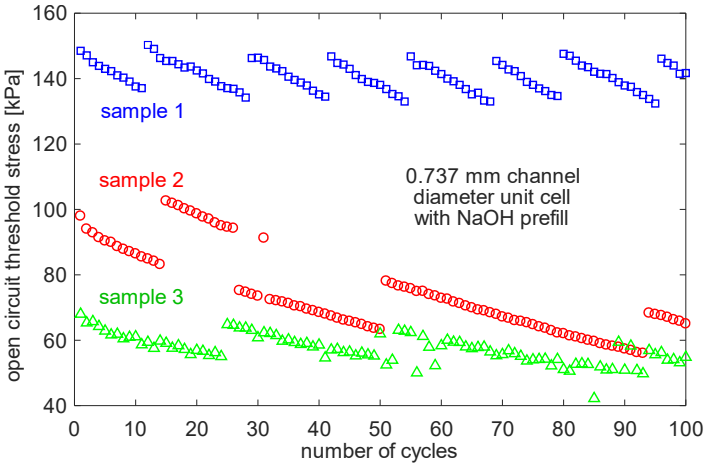

Figure S2. Open circuit threshold stress for unit cell samples using 0.737 mm microchannels and NaOH solution demonstrating staircase-type behavior of the threshold stress values.

References

[1] R.J. Larsen, M.D. Dickey, G.M. Whitesides, and D.A. Weitz, Viscoelastic properties of oxide-coated liquid metals. Journal of Rheology 53 (2009) 1305-1326.